

A Statistical Investigation of Internal Wave Propagation in the Northern South China Sea

Ping-Tung Shaw
Dept of MEAS, North Carolina State University
Box 8208
Raleigh, NC 27695-8208
Phone: (919)515-7276 fax: (919)515-7802 e-mail: pt_shaw@ncsu.edu

Award Number: N00014-10-1-0319

Award Number: N00014-10-1-0470

LONG-TERM GOALS

The long-term goal of this project is to predict the generation of internal waves over the ridges in the Luzon Strait and wave propagation across the northern South China Sea.

OBJECTIVES

The objective of this study is to provide a description of internal wave/tide propagation from the Luzon Strait to the edge of the continental shelf off China. Three issues are to be studied: 1) the relationship between the internal waves and the barotropic tides in the Luzon Strait, 2) temporal and spatial variations of internal wave properties during propagation across the deep basin of the northern South China Sea, and 3) wave transmission over the continental margin.

APPROACH

Guided by the characteristics of internal waves inferred from nonhydrostatic numerical simulation, time series analysis will be performed on simulated real-time data obtained from the Ocean Nowcast/Forecast System of Naval Research Laboratory during NLIWI. In the propagation region, wave fronts will be identified using depth integrated energy flux and the baroclinic velocity. The propagation speed of internal waves will be calculated. Trajectories of individual wave fronts will then be traced back to the Luzon Strait to pinpoint the location of wave generation and its dependence on the barotropic tides.

WORK COMPLETED

Internal solitary waves are represented by maxima in westward shallow flow and westward depth integrated energy flux. We have determined the positions of these maxima along 20.8°N in the NRL data during a two-month period in April-May, 2007. A comprehensive picture of internal wave propagation is obtained, covering an area from the Luzon Strait at 122°E to the edge of the continental shelf at 117°E. The result is verified by observation from the study of Alford, et al. (2010). The speed of westward propagating internal waves has been calculated. Cross-correlation of depth integrated energy flux and westward shallow velocity with the barotropic tides was obtained. From the wave

propagation speed and the time lag of individual waves after the barotropic tides, source regions of the internal waves were inferred.

The slope of the west ridge in the Luzon Strait is steeper on the east side than on the west side with a plateau in the center. In light of this asymmetric topography, we carried out a numerical study of internal wave generation on an asymmetric ridge. The results were compared with observation from Mascarene Plateau in the Indian Ocean.

RESULTS

Time series of depth integrated energy flux and surface baroclinic velocity along 20.8°N during April-May 2007 in the NRL data are examined. Figure 1 is a plot of the depth integrated energy flux in the time-longitude plane. Peaks in negative energy flux indicate westward propagation of internal waves in the northern South China Sea. Locations of wave fronts of internal solitary waves are determined from those peaks with a negative surface baroclinic velocity. Because the NRL model is hydrostatic, wave fronts in Figure 1 are not as sharp as those in the observation of Alford, et al. (2010). Nevertheless, the fine spatial resolution in the data reduces the uncertainties, and the trajectories of individual wave fronts can be determined with sufficient accuracy. Type-A and type-B waves are delineated by difference in arrival time of wave fronts at a particular location on successive days (24 hours for type-A waves and 24.84 hours for type-B waves). The result is shown in Figure 1 as solid and dashed lines, representing trajectories of type-A and type-B waves, respectively. All waves in the study of Alford, et al. (2010) can be identified in Figure 1, indicating that internal solitary waves in the northern South China Sea are adequately simulated by the NRL model.

Most type-A waves start east of 121°E , while type-B waves appear west of 120°E . At 20.8°N , the east ridge in the Luzon Strait is located at 121.8°E , while the west ridge has two peaks at 120.7 and 120.9°E (see Figure 3). Figure 1 suggests that type-A waves may have originated at the east ridge while type-B waves may have started from the west ridge.

The speed of westward wave propagation is inferred from Figure 1. To reduce the error in speed calculation, we have shifted the time coordinate for each trajectory by an integer multiple of the tidal period (24 hours for type-A waves and 12.42 hours for type-B waves) so that all trajectories have a common origin. The result for type-A waves identified during the study period is shown in Figure 2. The trajectories can be fitted by a line between 117.5°E and 121°E , confirming that type-A waves arrive at a particular location at the same time each day. The speed estimated from the slope is 3.0 m/s for type-A waves, consistent with that observed by Alford, et al. (2010). Similar analysis has been performed for type-B waves (not shown). The speed is between 2.5 and 3.0 m/s , slightly slower than that of type-A waves. Noticeable slowdown is observed west of 117.5°E when type-B waves reach the continental slope. Again the speed is consistent with that obtained from mooring data.

The lag time between the depth integrated energy flux at 119°E and velocity of the barotropic tide is calculated from correlation analysis. Multiple lag times differing by an integer multiple of the tidal period are present. Speeds required for internal wave to travel from the ridges in Luzon Strait to 119°E are obtained from the lag times. Only two scenarios are possible: a speed of 2.5 m/s for waves originating at 120.9°E at the semidiurnal period and a speed of 3.0 m/s for waves originating at 121.8°E at the diurnal period. In both cases, westward baroclinic velocity starts with westward tidal flow. The result confirms that type-A and type-B waves originate at the east ridge and the east side of

the west ridge, respectively. A cross-sectional view of the baroclinic velocity is shown in Figure 3. Wave beams at shallow depths show internal wave generation from two ridges. These wave beams can be identified in Figure 1 at later times. Generation of diurnal and semidiurnal waves at the two ridges is also demonstrated by energy density averaged over a fortnightly period starting from April 25 (Figure 4). Generation of diurnal wave energy from the east ridge and the semidiurnal wave energy from the west ridge is clearly demonstrated.

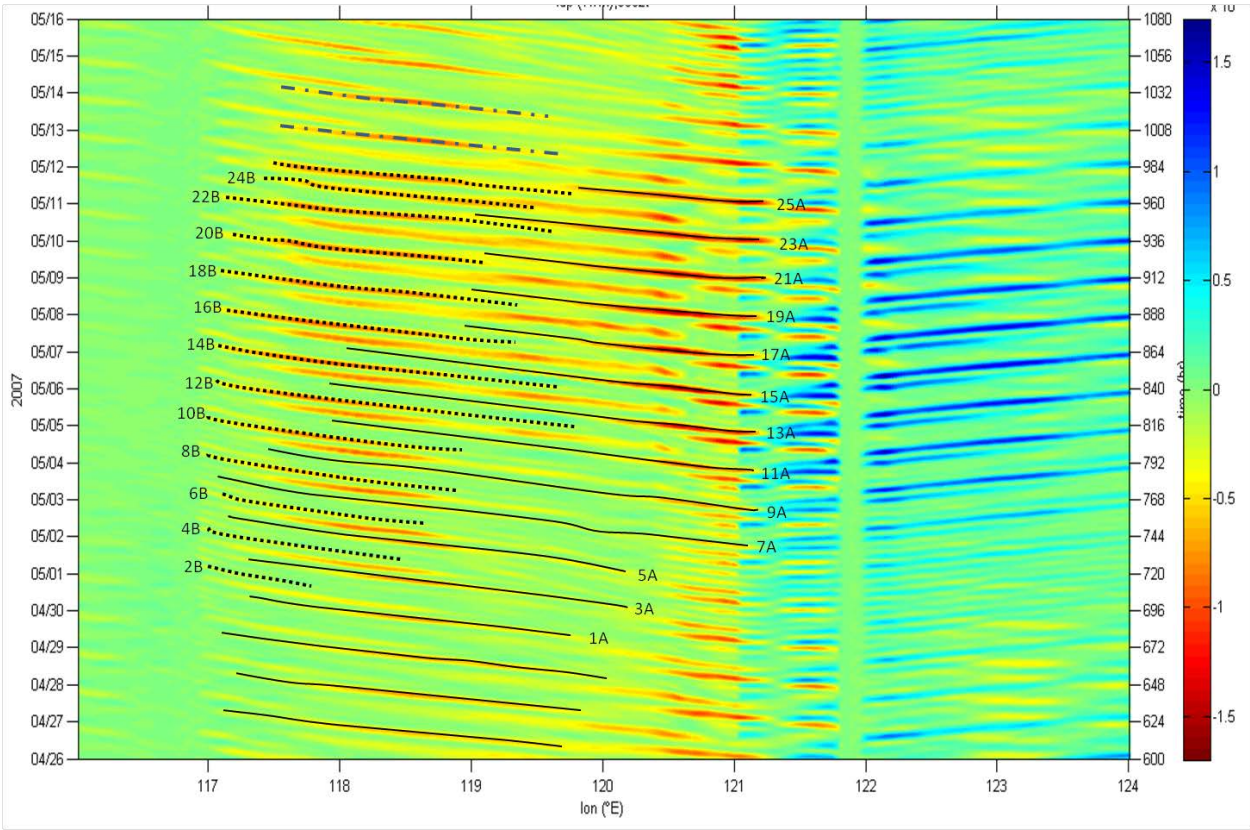


Figure 1. Contour plot of vertically integrated internal wave energy flux in J/m^2 from April 26 to May 16, 2007. Each wave front is indicated by a sequential number followed by the type of wave. Type-A and type-B waves are determined by lag times of 24 hr and 24.84 hours, respectively.

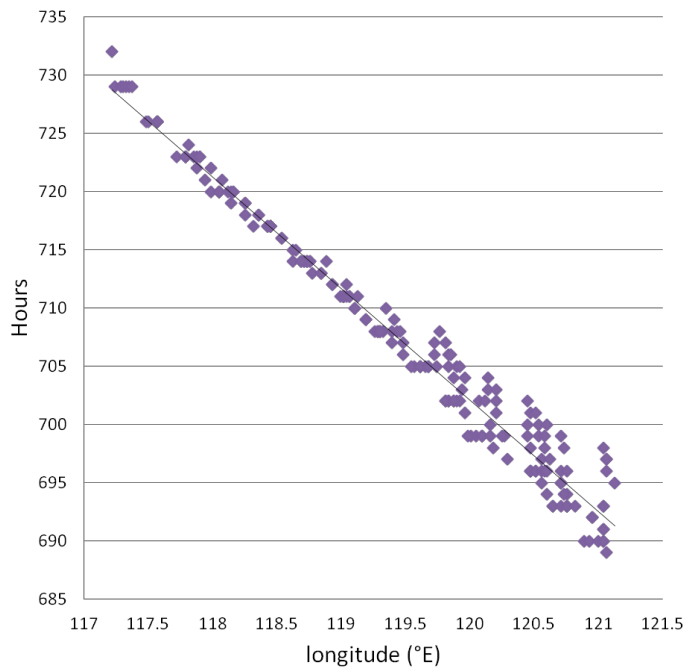


Figure 2. Locations of type-A waves identified in Figure 1. The time coordinate for each wave is shifted by an integer multiple of 24 hours so that all trajectories have the same time origin. The line represents a speed of 3.0 m/s.

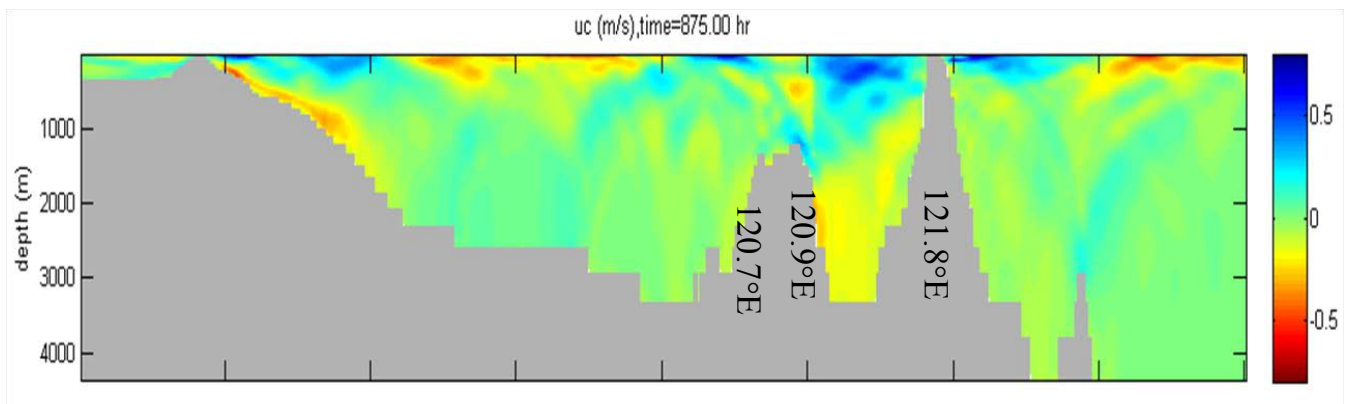


Figure 3. A snap shot of baroclinic velocity along 20.8°N . Waves emit from the east ridge at 121.8°E and the east side of the west ridge at 120.9°E .

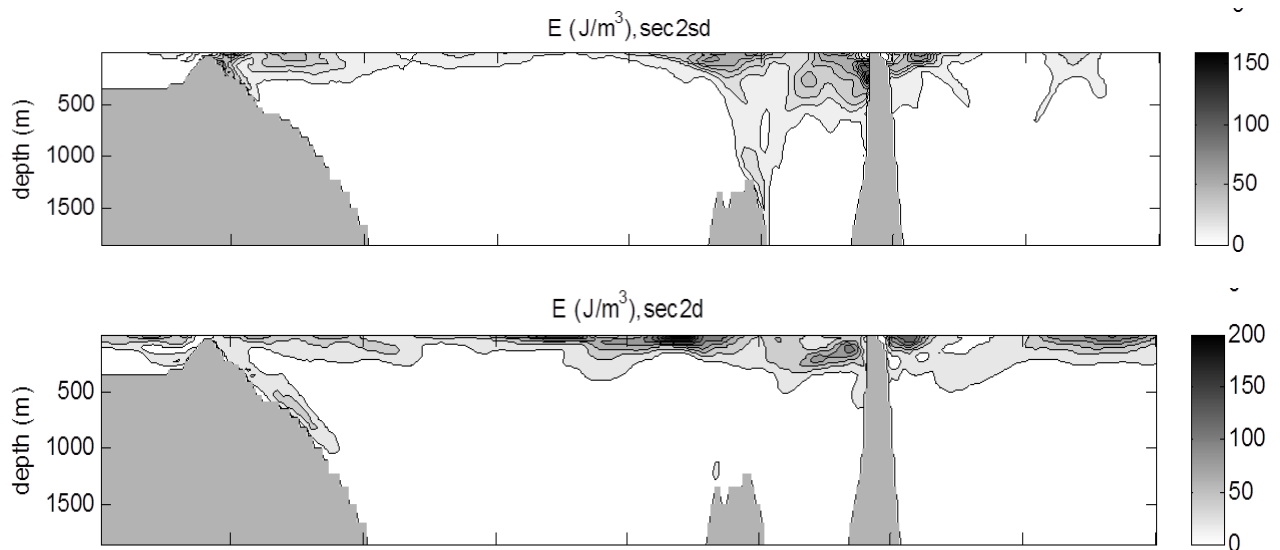


Figure 4. Energy density of internal wave along 20.81°N at the semidiurnal period (top panel) and the diurnal period (bottom panel). Energy density is average over 14 days, the fortnightly period. Westward propagating waves originate at the east face of the west ridge at the semi-diurnal period and the east ridge at the diurnal period.

The west ridge has a steeper slope on the east side (Figure 3). Effects of an asymmetric ridge on internal wave generation are studied using the process oriented model of Shaw and Chao (2006). Figure 5 shows energy density of internal waves forced by the semidiurnal tide. Waves are generated from the supercritical side of the ridge, confirming that the steeper east side of the west ridge is the main source of semidiurnal waves.

IMPACT/APPLICATIONS

All internal waves observed in the study of Alford, et al. (2010) are identified in the NRL data, indicating that the NRL simulation, albeit being hydrostatic, adequately reproduces the internal wave field in the northern South China Sea. Regions of wave generation can be located because of the fine spatial resolution and comprehensive spatial coverage in the NRL data, especially in the wave generation region. The result from this study indicates that the process of wave generation and propagation in the northern South China Sea can be resolved using NRL data. Process studies such as the one shown in Figure 5 provide further understanding of the generation mechanism. Continuing this analysis will produce a comprehensive picture of internal waves in the northern South China Sea. Mooring measurements are not likely to achieve sufficient spatial resolution of the internal wave field in the Luzon Strait. Nonhydrostatic simulation is too costly for real-time simulation. Using the NRL data set is the most practical approach for studying generation of internal waves in the northern South China Sea and its fortnightly, seasonal, and interannual variations.

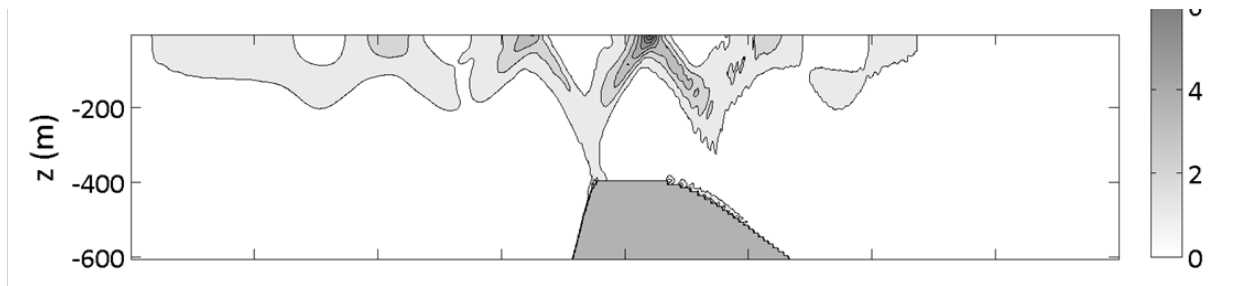


Figure 5. Energy density (J/m^3) of internal wave generated from an asymmetric ridge in a nonhydrostatic model. The half widths of the ridge are 15 km and 78 km on the two sides of the ridge, respectively. Contour interval is $1 J/m^3$. The scale of the horizontal axis is 400 km. Wave energy is mostly generated on the supercritical slope on the left.

RELATED PROJECTS

Award N00014-10-1-0470 is for support of a graduate student (Ying-Jung Chen) to work on this project .

REFERENCES

- Alford, M.H., R.-C. Lien, H. Simmons, J. Klymak, S. Ramp, Y. J. Yang, D. Tang, and M.-H. Chang (2010) Speed and evolution of nonlinear internal waves transiting the south china sea, *Journal of Physical Oceanography*, 40, 1338-1355. doi: 10.1175/2010JPO4388.1
- Shaw, P. and S. Chao (2006), A nonhydrostatic primitive-equation model for studying small-scale processes: An object-oriented approach, *Cont. Shelf Res.*, 26(12-13), 1416-1432, doi: 10.1016/j.csr.2006.01.018.

PUBLICATIONS

- Angus, M., (2012) The effect of asymmetrical topography on the generation of internal waves. MS Thesis, Department of Marine, Earth and Atmospheric Sciences, North Carolina State University, Nov. 2012. [published, non-refereed]